FEBS Letters 589 (2015) 2401–2408

FEBS Letters

journal homepage: www.FEBSLetters.org

Phosphoproteomic analysis of the mouse brain mu-opioid (MOP) receptor

Lionel Moulédous [a], Carine Froment [a], Odile Burlet-Schiltz [a], Stefan Schulz [b], Catherine Mollereau [a,*]

[a] Institut de Pharmacologie et Biologie Structurale CNRS/Université de Toulouse, 205 route de Narbonne, 31077 Toulouse, France
[b] Institute of Pharmacology and Toxicology, Jena University Hospital, Friedrich Schiller University Jena, Drackendorfer Strasse 1, 07747 Jena, Germany

ARTICLE INFO

Article history:
Received 26 May 2015
Revised 3 July 2015
Accepted 20 July 2015
Available online 29 July 2015

Edited by A. Chattopadhyay

Keywords:
G-protein coupled receptor (GPCR)
Opioid
Phosphorylation
Proteomic

ABSTRACT

Many in vitro data have shown that the efficacy of several opioid drugs is correlated with differential mu-opioid (MOP) receptor phosphorylation. Label-free semiquantitative on-line nanoflow liquid chromatography–tandem mass spectrometry (nanoLC–MS/MS) analyses were performed to compare the endogenous MOP receptor phosphorylation patterns of mice administered with morphine, etonitazene and fentanyl. The analysis identified S363, T370 and S375 as phosphorylated residues in the carboxy-terminus. Only T370 and S375 were regulated by agonists, with a higher propensity to promote double phosphorylation for high efficacy agonists. Our study provides confirmation that differential agonist-driven multi-site phosphorylation of MOP receptor occurs in vivo and validate the use of MS to study endogenous GPCR phosphorylation.

1. Introduction

Opioids, acting through G-protein coupled receptors (GPCR), are the most effective drugs for the treatment of moderate to severe pain but improving their use is still a matter of concern as many undesirable effects limit their clinical utility. Moreover prolonged opiate administration is associated with tolerance and pain hypersensitivity [1–3]. Phosphorylation of the intracellular domain of GPCR is a key component of the regulation of their function, playing a well-established role in desensitization and internalization [3,4]. Recent studies indicate that differential agonist/cell-dependent phosphorylation patterns behave as signaling barcodes driving the specificity of cell response [5–8]. This mechanism could contribute to the differential effects of opioid drugs used in pain management, as suggested recently [9]. However, the analysis of MOP receptor phosphorylation has been so far restricted to selected phosphorylation sites by using phospho-specific antibodies and thus a full characterization of the in vivo phosphorylation pattern of the receptor upon stimulation by different agonists is still lacking.

In vitro MOP receptor phosphorylation has been studied by site-directed mutagenesis [10,11], phosphosite-specific antibodies [12] and, more recently, mass spectrometry (MS) analysis [13–17]. Overall, data indicate that variation in the efficacy of several opioid drugs in terms of desensitization, arrestin recruitment and internalization is correlated to differential MOP receptor phosphorylation, involving diverse GRK or second-messenger kinases [15,18–20]. Phosphorylation of the MOP receptor occurs primarily at S363 and within a cluster of serine and threonine residues (^{370}TREHPSTANT^{379}) in the cytoplasmic tail (Fig. 1). Rodent S363 (or S365 in human) is constitutively phosphorylated and not subject to regulation by agonists in transfected cells [11,12,16,17,21], while a sequential and agonist-dependent differential phosphorylation occurs in the ^{370}TREHPSTANT^{379} cluster. S375 is phosphorylated upon stimulation with both partial agonists such as morphine and high efficacy agonists such as DAMGO, but only the latters are able to promote additional phosphorylation on T370, T376 and T379 [15,22]. The demonstration of poly-phosphorylation on single ^{370}TREHPSTANT^{379} peptides was given by mass spectrometry analyses that identified peptides doubly or triply phosphorylated on both T370 and S375, and another residue [16,17]. In cell lines, the phosphorylation of S375 by morphine is proposed to be mediated for a significant part by GRK5 while the phosphorylation of S375, T370, T376 and T379 by DAMGO involves GRK2/3 isoforms

---

Abbreviations: MOP receptor, mu-opioid receptor; NanoLC–MS/MS, on-line nanoflow liquid chromatography–tandem mass spectrometry

Author contributions: Performed the research: L.M., C.F., S.S. and C.M. Designed the research study: C.M., L.M. and S.S. Contributed essential reagents or tools: S.S and O.B.S. Analyzed the data: C.M., L.M., C.F. and O.B.S. Wrote the paper: C.M., L.M. and S.S. All authors have seen the final manuscript.

[*] Corresponding author.

E-mail addresses: Stefan.Schulz@med.uni-jena.de (S. Schulz), catherine.mollereau-manaute@ipbs.fr (C. Mollereau).

http://dx.doi.org/10.1016/j.febslet.2015.07.025

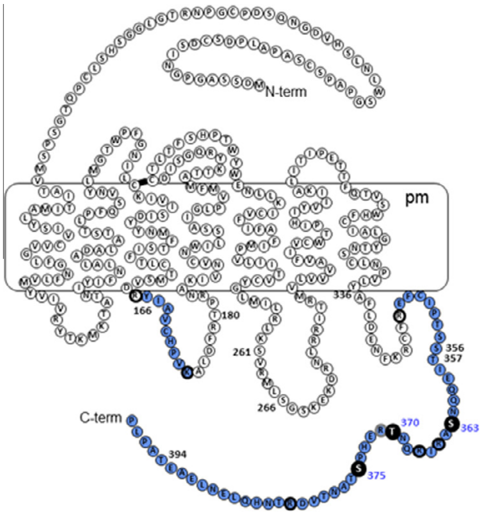

Theo mass.	MC	Position		Sequence	P-residue
1028.55	0	166-174	il2	YIAVCHPVK	
1909.88	0	349-365	C-term	EFCIPTSSTIEQQNSAR	
1989.85	0	349-365	C-term	EFCIPTSSTIEQQNSAR	S363
1225.57	0	372-382	C-term	EHPSTANTVDR	
1305.54	0	372-382	C-term	EHPSTANTVDR	S375
1804.79	1	368-382	C-term	QNTREHPSTANTVDR	T370
1884.75	1	368-382	C-term	QNTREHPSTANTVDR	T370 and S375
1775.87	0	383-398	C-term	TNHQLENLEAETAPLP	

Fig. 1. Mass spectrometry coverage of the mouse brain MOP receptor sequence. The schema represents the secondary structure of the mouse MOP receptor. Colored symbols indicate the protein sequence covered by nanoLC–MS/MS. The phosphorylated residues identified by nanoLC–MS/MS are represented in black symbols with white characters, and are numbered in blue. Additional putative phosphoacceptor sites reported in the literature are numbered in black. Thick outlined circles indicate the trypsin cleavage sites, with light gray outline for missed cleavages. pm, plasma membrane. The table gives the list of the MOP receptor peptides identified by nanoLC–MS/MS with a Mascot score >24. Theo. mass., theoretical mass (Da); MC, missed cleavage; il, intracellular loop; C-term; carboxy-terminal intracellular tail.

[15,18]. Mutation in the ^{370}TREHPSTANT^{379} sequence, especially S375, results in impaired β-arrestin recruitment and MOP receptor internalization [11,15,16], and in loss of morphine, but not DAMGO, -induced desensitization of cAMP and ERK pathways [23]. However, no effect on met-enkephalin-induced GIRK desensitization was recently reported, thus questioning the role of this cluster in desensitization [22,24].

In vivo MOP receptor phosphorylation is less well documented. Immunoprecipitation of MOP receptor from the mouse brain [25], followed by phosphosite-specific immunodetection, demonstrated that the endogenous receptor is phosphorylated on S375 upon morphine, fentanyl or etonitazene administration, with additional phosphorylations on T370 and T379 only in the case of fentanyl and etonitazene treatment [9,18,26]. Constitutive phosphorylation of S363, without regulation by agonist treatment, was also evidenced [21]. An increase in MOP receptor phosphorylation within the striatum of mice administered with fentanyl has also been revealed by immunochemistry using an antibody raised against a peptide with double phosphorylation on T370 and S375 [27]. Studies in GRK knock-out mice indicate that GRK5 is selectively involved in morphine-induced phosphorylation of S375 [18] and that GRK3 contributes to S375 phosphorylation induced by fentanyl and, to a lesser extent, by morphine [9].

Mass spectrometry has been used as an alternative to phospho-site specific antibodies to study GPCR phosphorylation in heterologous cellular models [5,7,13–17]. It is a powerful technology offering the advantage over antibodies to allow the analysis of all the putative phosphoacceptor sites and the identification of new post-translational modifications, as well as the demonstration of multi-site phosphorylation on a single receptor. However its usefulness for the characterization of low abundance native receptors is only beginning to be evaluated [9]. In the present study we have applied a mass spectrometry-based approach to analyze the endogenous phosphorylation pattern of MOP receptor following acute administration of different classes of opioid drugs in mice.

2. Methods

2.1. Materials

Morphine hydrochloride was obtained from Merck (Darmstadt, Germany), fentanyl citrate from Rotexmedica (Trittau, Germany), and etonitazene hydrochloride from Sigma–Aldrich (Steinheim, Germany). Drugs were dissolved in physiological saline and injected subcutaneously (s.c.) in a volume of 10 ml kg^{-1}.

2.2. Animal welfare and ethical statement

The C57BL6/J mice were obtained from Charles River (Sulzfeld, Germany). Knock-in mice expressing the phospho-deficient (S375A) MOP receptor mutant were previously described [26]. Animals were housed under a 12 h light–dark cycle with ad libitum access to food and water. All animal care and experimental procedures were approved by the Thuringian state authorities and complied with EC regulations for the care and use of laboratory animals. All studies involving animals are reported in accordance with the ARRIVE (Animal Research: Reporting In Vivo Experiments) guidelines. A total of 14 mice were used.

2.3. In vivo MOP receptor immunoprecipitation

30 min after s.c. administration of saline, morphine (10 mg kg^{-1}), fentanyl (0.1 mg kg^{-1}) or etonitazene (0.1 mg kg^{-1}), mice were anesthetized by isoflurane, killed by cervical dislocation, and brains (without cerebellum) were quickly dissected and processed for immunoprecipitation with the phosphorylation-independent rabbit monoclonal anti-MOP receptor antibody (UMB-3) as previously described [9,25].

2.4. SDS–PAGE and immunoblotting

UMB-3 immunoprecipitates from one brain per condition, including a control with no brain extract (UMB-3 alone), were boiled for 5 min at 100 °C and then alkylated in 90 mM iodoacetamide for 30 min in the dark. 2 μl from each brain extract were pooled and separated by SDS–PAGE on 10% polyacrylamide gels. The UMB-3 immunoprecipitates intended for MS analysis were run on the same gel. The part of the gel for immunoblotting was transferred to PVDF membrane and processed under standard conditions in Tris–Buffered Saline (20 mM Tris–HCl, pH 7.5, 137 mM NaCl) containing 0.2% Tween and 5% non-fat milk. The MOP receptor was detected with a guinea pig anti-MOP receptor antibody (Neuromics, USA) followed by a peroxydase-conjugated goat anti-guinea pig antibody (Jackson Immunoresearch Laboratories, USA) by using the ECL2 Western blotting substrate (Thermo Fisher Scientific, France).

Immunoblotting from brains of wild-type and phospho-deficient S375A MOP receptor mice injected (30 min, s.c.) with etonitazene 0.1 mg kg^{-1} were performed as previously described [26]. The blot was probed with guinea pig anti-pT370 and anti-p375, and with phosphorylation-independent guinea pig anti-MOP receptor antibody to control gel loading, including a stripping step between each blot.

2.5. NanoLC–MS/MS analysis

Gels were stained with colloidal Coomassie blue for 24 h. A band was excised at the molecular weight of the MOP and subjected to in-gel tryptic digestion using modified porcine trypsin (Promega, France) at 20 ng μl^{-1}. The dried peptide extracts were then analyzed by on-line nanoLC using an Ultimate 3000 System (Dionex, Amsterdam, The Netherlands) coupled to an ETD-enabled LTQ Orbitrap Velos mass spectrometer (Thermo Fisher Scientific, Bremen, Germany) as previously described [17] except for the MS/MS acquisition mode which was an alternative decision tree-driven collision-induced dissociation (CID)/electron transfer dissociation (ETD) fragmentation acquisition instead of two consecutive CID and ETD acquisitions. The survey scan MS was performed in the Orbitrap on the 300–2000 m/z mass range with the resolution set to a value of 60000 at m/z 400. The 20 most intense ions per survey scan were selected for subsequent CID/ETD fragmentation, and the resulting fragments were analyzed in the linear trap (LTQ). The settings for the data-dependent decision tree-based CID/ETD method were as follows: ETD was performed instead of CID if charge state was 3 and m/z less than 650, or if the charge state was 4 and the m/z less than 900, or if the charge state was 5 and the m/z less than 950. ETD was performed for all precursor ions with charge states >5. The normalized collision energy was set to 35% for CID. The reaction time was set to 100 ms and supplemental activation was enabled for ETD. Triple technical replicates were performed in some conditions.

2.6. Database search and label-free determination of MOP receptor phosphopeptide relative abundance ratio

Peak list extraction from Xcalibur raw files was automatically performed using Proteome Discoverer software (version 1.4, Thermo Fisher Scientific). The parameters set for creation of the peak lists were: parent ions in the mass range 300–5000 and no grouping of MS/MS scans. The non-fragmented filter was used to simplify ETD spectra with the following settings: the precursor peak was removed within a 4-Da window, charged reduced precursors were removed within a 2-Da window, and neutral losses from charged reduced precursors were removed within a 2-Da window (the maximum neutral loss mass was set to 120 Da). Peak lists were searched against SwissProt database with taxonomy *Mus musculus* (16611 sequences) and using Mascot software (version 2.3.01, Matrix Science, London, UK). Cysteine carbamidomethylation was set as a fixed modification and methionine oxidation, N-terminal acetylation and serine/threonine/tyrosine phosphorylations as variable modifications. Up to three missed trypsin cleavages were allowed. Mass tolerances in MS and MS/MS were set to 10 ppm and 0.6 Da, respectively. Mascot results were parsed with the in-house developed software Mascot File Parsing and Quantification (MFPaQ) version 4.0 [28], and protein hits were automatically validated if they satisfied one of the following criteria: identification with at least one top ranking peptide of a minimal length of six amino acids and with a Mascot score higher than the identity threshold at $P = 0.001$ (99.9% probability) or at least two top ranking peptides each of a minimal length of six amino acids and with a Mascot score higher than the identity threshold at $P = 0.05$ (95% probability). The peptides of MOP receptor were considered as valid if their Mascot ion scores were higher than 24 (P value <0.05), if not the identification was confirmed by manual interpretation of corresponding MS/MS data. The phosphorylation site localization of identified phosphopeptides was performed by phosphoRS algorithm 3.1 [29] implemented in Proteome Discoverer. A site localization probability of at least 0.75 was used as the threshold for the phosphoresidue localization. Peak areas were automatically measured from extracted ion chromatograms of each peptide (sum of all observed charge states) in the nanoLC–MS raw file using the label-free module of MFPaQ software. To calibrate the amounts of MOP receptor in the different conditions, normalization was performed based on the sum of the extracted ion chromatogram areas of all identified MOP receptor peptides. In the case where a peptide was missing in one sample, a value corresponding to the peak area of the peptides of the lowest abundance (1st percentile) among all the peptides identified in the sample was assigned to the missing data.

3. Results

3.1. NanoLC–MS/MS analysis of MOP receptors from mouse brain

The UMB-3 antibody has been previously demonstrated to specifically immunoprecipitate the MOP receptor from mouse brain as a broad band in the 70–80kDa range [25,26]. It was efficient enough to enable detection of MOP receptor peptides by mass spectrometry from only one mouse brain [9]. This prompted us to characterize the in vivo phosphorylation patterns of MOP receptors after treatment of mice (30 min, s.c.) with saline, morphine (10 mg kg^{-1}), fentanyl (0.1 mg kg^{-1}) or etonitazene (0.1 mg kg^{-1}). An example of SDS–PAGE separation of UMB-3 immunopurified MOP receptor is given in Fig. 2, as well as the corresponding Western blot run on the same gel and loaded with a small amount of sample and with a control without brain extract. A specific band was visible on the immunoblot at the MOP receptor expected size. After in-gel tryptic digestion of the excised band corresponding to the position of the receptor, nanoLC–MS/MS decision tree-driven CID/ETD analyses and Mascot database searches, including putative phosphorylation modification, identified the MOP receptor sequence with 15% coverage. This included half of the 2nd intracellular loop (il2) and nearly all the amino acids of the C-terminal tail allowing the characterization of 12 putative phosphorylation sites (Fig. 1). As expected because of the abundance of lysine and arginine residues in il1 and il3, resulting in the generation of short 2–3 amino acid-long peptides, these regions were not covered. Also, the peptide ^{175}ALDFR^{179} in il2, although always detected, was not considered in the study because of its low Mascot score.

Overall, 7 among the 11 residues reported in the literature to be potentially phosphorylated in MOP receptors were covered. In the C-terminal part, unphosphorylated and monophosphorylated forms of S363 (Fig. 3A) and S375 (Fig. 3C) containing peptides were identified by CID/ETD fragmentation analyses. As T370 is surrounded by two arginines, only phosphorylated forms of T370 containing peptides could be detected owing to miscleavages due to phosphate hindrance to trypsin activity (Figs. 1 and 3B). Interestingly, double phosphorylation on T370 and S375 was unambiguously identified on the ^{368}QNTREHPSTANTVDR^{382} peptide (Fig. 3D). The ^{166}YIAVCHPVK^{174} peptide in il2 and the ^{383}TNHQLENLEAETAPLP^{398} peptide at the C-terminal extremity, which were consistently detected in all conditions, were never found phosphorylated. Also, no other phosphorylation than S363 was detected in the ^{349}EFCIPTSSTIEQQNSAR^{365} peptide. In samples from agonist-treated mice, MS analyses identified the same unphosphorylated and phosphorylated peptides as in saline mice,

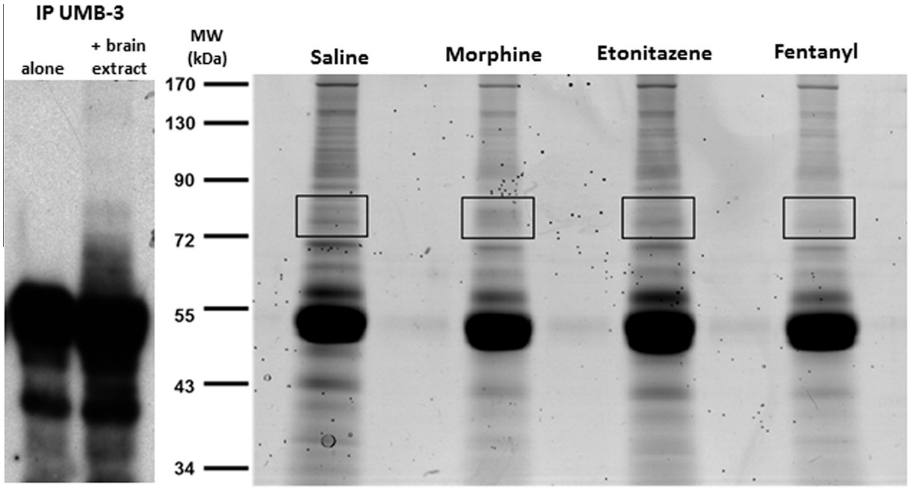

Fig. 2. Western blot image (left) and Coomassie blue-stained gel (right) of UMB-3-immunopurified MOP receptor from mouse brain. The immunoprecipitated material from brain of mice injected (30 min, s.c.) with saline, morphine (10 mg kg^{-1}), etonitazene (0.1 mg kg^{-1}) or fentanyl (0.1 mg kg^{-1}) was separated by SDS–PAGE. Left, immunoblot using anti-MOP antibody. The "alone" lane corresponds to a control immunoprecipitation performed in the absence of brain extract. The "+ brain extract" lane corresponds to a pool of small aliquots of each extract. Right, Coomassie blue staining of the immunoprecipitated material. Rectangles delimitate the pieces of gel containing the MOP receptor and excised for nanoLC–MS/MS analysis.

without clear evidence of the presence of additional phosphorylated species. However, agonist treatment increased the abundance of several phosphorylated peptides compared to saline.

3.2. Relative label-free quantification of agonist-induced phosphorylation of endogenous MOP receptor

The label-free module of the MFPaQ software was used to calculate the relative abundance of phosphorylated and unphosphorylated peptides in the agonist-treated conditions relative to saline (Fig. 4). No difference between saline and agonist-treated groups was observed for the S363-phosphorylated form of ^{349}EFCIPTSSTIEQQNSAR^{365} or the T370-phosphorylated form of ^{368}QNTREHPSTANTVDR^{382}, indicating that these peptides were constitutively phosphorylated. In contrast, the agonists were found to slightly increase the phosphorylation on S375 and to exhibit a differential propensity for driving double phosphorylation on S375 and T370. The S375-phosphorylated form of the ^{372}EHPSTANTVDR^{382} peptide was 1.9 ± 0.6, 2.3 ± 0.8 and 2.6 ± 0.9-fold more abundant in etonitazene, morphine and fentanyl treated mice than in saline group, respectively. A significant increase in the abundance of pT370/S375 diphosphorylated ^{368}QNTREHPSTANTVDR^{382} peptide was observed in mice injected with fentanyl (×2.7 ± 0.1) and etonitazene(×6.2 ± 0.3), but not in the morphine group(×1.5 ± 0.7). Since the amount of receptor species with monophosphorylation on T370 remained unchanged in all conditions, it can be concluded that diphosphorylated species result from the phosphorylation of T370 on a receptor previously phosphorylated on S375. This hierarchical phosphorylation was confirmed in phospho-deficient S375A MOP receptor mice administered with etonitazene, in which the loss of S375 phosphorylation was accompanied by a decrease in T370 phosphorylation, as compared to wild-type mice (Fig. 5). Our MS analysis thus confirms the differential capacity of agonists to induce MOP receptor phosphorylation and provides evidence that high efficacy opioids trigger multiphosphorylation on a single peptide.

4. Discussion

This work is the first detailed mass spectrometry analysis of the in vivo phosphorylation of a brain GPCR. To our knowledge, only one other study has previously reported the MS identification of phosphorylation sites in a native GPCR, the N-formyl peptide receptor (FPR1), but from ex vivo stimulated human blood neutrophils [30]. The present phosphoproteomic analysis of native MOP receptor not only allowed an accurate identification of the residues phosphorylated in vivo and their regulation by agonist treatments, but also confirmed that differential agonist-induced multiple phosphorylation on a single receptor occurs in vivo.

The analysis covered half of the putative phosphorylation sites present in the intracellular domains of the mouse endogenous MOP receptor and identified S363, T370 and S375 as phosphorylated residues, in accordance with MS analyses in transfected cellular models [13,16,17]. Only the phosphorylation of T370 and S375 was increased by agonist administration.

In contrast to in vitro MS studies reporting phosphorylation of the ^{354}TSST^{357} motif upon agonist stimulation of transfected mouse or rat receptors [13,16], we did not identify phosphorylated residues other than S363 in the ^{349}EFCIPTSSTIEQQNSAR^{365} peptide from the endogenous mouse MOP receptor. Though differences in detection sensitivity between native preparation and overexpressed receptors cannot be excluded, this suggests that the ^{354}TSST^{357} motif is not a primary phosphorylation cluster in vivo. In this sense, alanine mutations within this motif show unconsistent results in the literature: no effect on MOP receptor phosphorylation level [11,31], desensitization [24,31] and internalization [16]; decreased phosphorylation and desensitization in the case of the rat S355A/T357A receptor mutant [32]; impact on agonist dissociation kinetics [24].

In agreement with the literature [20], phosphorylation of S363 was not found to be regulated by in vivo administration of morphine, etonitazene and fentanyl, indicating constitutive phosphorylation of this residue in native MOP receptors. Upon administration of morphine, etonitazene or fentanyl, a higher proportion of MOP receptor phosphorylated on S375 and doubly phosphorylated on S375 and T370 was detected compared to animals injected with saline, whereas the proportion of MOP receptor only phosphorylated on T370 was unchanged. Along with the decrease of etonitazene-induced T370 phosphorylation observed in phospho-deficient S375A MOP receptor mice, these results indicate that the hierarchical multi-site phosphorylation involving a primary step of S375 phosphorylation and described in cellular models [15] also occurs in vivo.

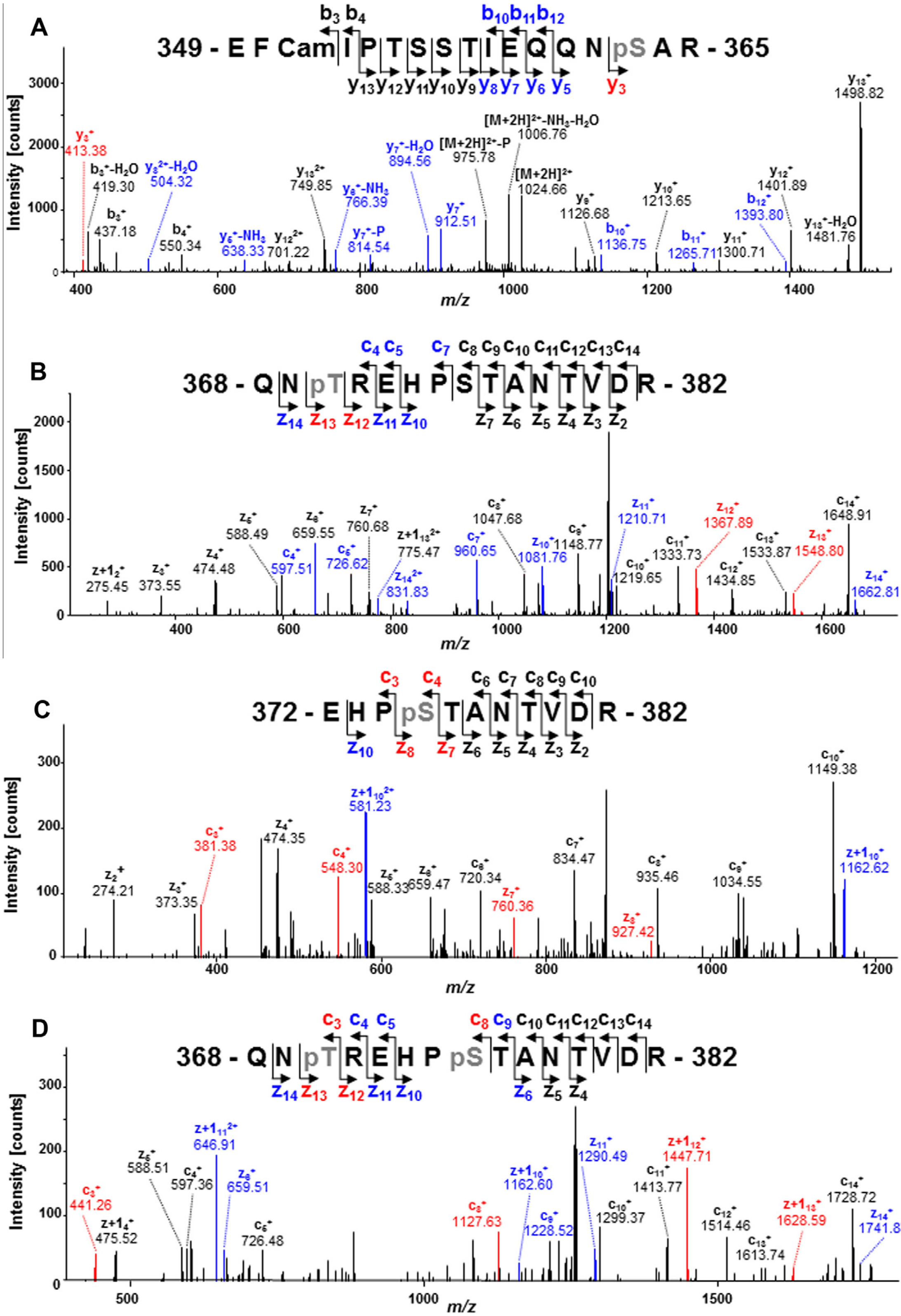

Fig. 3. NanoLC–MS/MS analysis of MOP receptor phosphorylation. (A) The CID MS/MS spectrum of the monophosphorylated peptide, 349-EFCamIPTSSNIEQQNpSTR-365 (doubly charged precursor ion, MH^{2+}, at *m*/*z* 1024.4419) displays series of b- and y-ions indicating that S363 is phosphorylated. (B) The ETD MS/MS spectrum of the monophosphorylated peptide, 368-QNpTREHPSTANTVDR-382 (triply charged precursor ion, MH^{3+}, at *m*/*z* 602.6024) displays series of c- and z-ions indicating that T370 is phosphorylated. (C) The ETD MS/MS spectrum of the monophosphorylated peptide, 372-EHPpSTANTVDR-382 (triply charged precursor ion, MH^{3+}, at *m*/*z* 436.1857) displays series of c- and z-ions indicating that S375 is phosphorylated. (D) The ETD MS/MS spectrum of the diphosphorylated peptide, 368-QNpTREHPpSTANTVDR-382 (triply charged precursor ion, MH^{3+}, at *m*/*z* 629.2578) displays series of c- and z-ions indicating that T370 and S375 are phosphorylated. For all spectra, phosphorylation site-determining ions and the corresponding peaks are highlighted in red and those which confirm the phosphorylation localization and exclude other potential sites are indicated in blue. P: loss of H3PO4 from sequence ions. pS, pT: phosphorylated serine or threonine residues. Cam: carbamidomethylated cysteine residue.

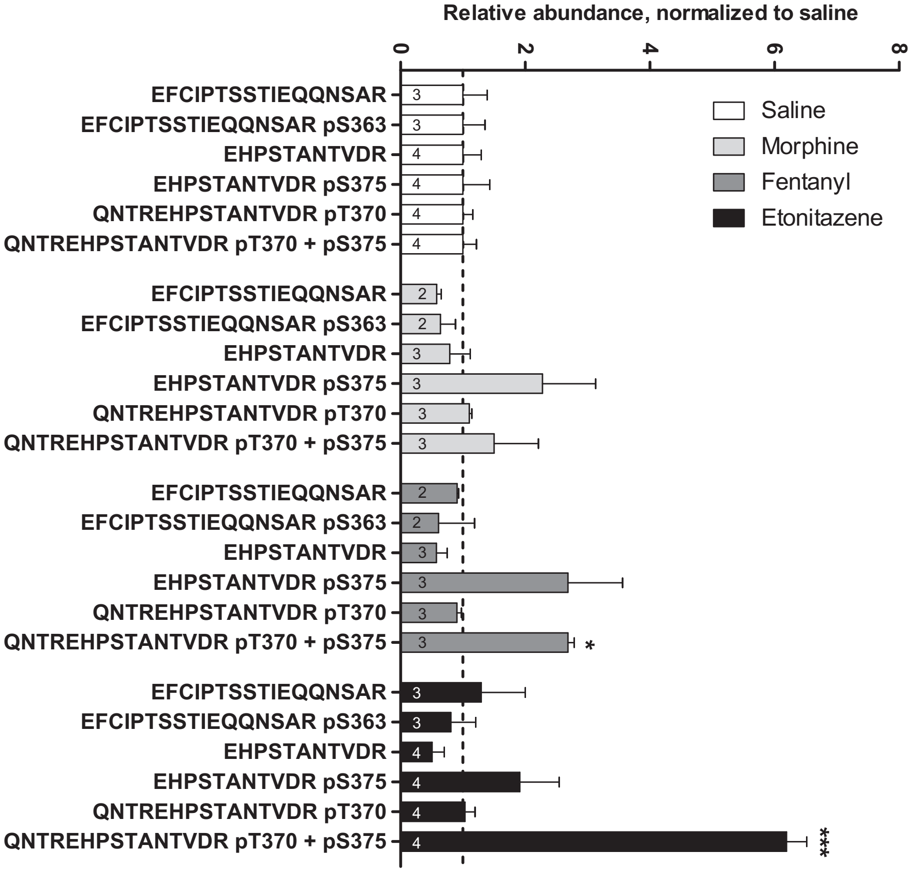

Fig. 4. Relative abundance ratio (compared to saline) of unphosphorylated, monophosphorylated and diphosphorylated MOP receptor peptides identified in mice treated (30 min, s.c.) with saline ($n = 4$), morphine 10 mg kg^{-1} ($n = 3$), fentanyl 0.1 mg kg^{-1} ($n = 3$) or etonitazene 0.1 mg kg^{-1} ($n = 4$). Relative quantification of peptides was performed with the label-free module implemented in the MFPaQ v4.0 software. To enable comparison between samples, the peak area of each peptide in a sample was normalized to the sum of the extracted ion chromatogram area of all identified MOP receptor peptides. Bars correspond to the relative ratio of normalized peak intensities of each group over saline group, and are expressed as mean ± SEM of the number of mice extracts in which the peptide was detected (numbers indicated in each bars). $^{*}P < 0.05$, $^{***}P < 0.001$, different from the corresponding peptide in saline condition (1-way ANOVA followed by Dunnett's post-test).

Among the three agonists, etonitazene was the most efficient to induce double phosphorylation whereas morphine effect was not statistically significant, confirming in vitro studies reporting that higher efficacy agonists induce a higher level of multi-site phosphorylation [15]. However, additional phosphorylations on residues T376 and T379 have been identified by phosphosite-specific antibodies in cells [15] and/or in vivo [9], and triple phosphorylation on the ^{366}IRQNTREHPSTANTVDR^{382} peptide was detected by MS analysis, however upon a prolonged agonist treatment (180 min) of recombinant cells [16]. Our mass spectrometry analysis did not clearly identify additional phosphorylation on T376 or T379, pointing to the necessity of improving the sensitivity of the method for detecting the presence of low-abundant triple (or more) phosphorylated peptides in vivo. Applying SRM (single reaction monitoring) targeted proteomics or phosphopeptide enrichment could be envisaged, but a more prolonged treatment with agonists or the use of higher doses could also potentially increase the amount of multiphosphorylated species.

Beside the major phospho-residues identified in the present study, a number of other putative phosphorylation sites have been described in the literature on the basis of mutagenesis studies or phospho-site immunodetection in recombinant cell models. Among them, two are covered by our analysis but were not found to be phosphorylated in the native receptor: Y166 in the DRY motif, which necessitates costimulation of the cells by DAMGO and EGF to be phosphorylated and contributes to reduce G-protein coupling [33], and T394, the mutation of which induces a loss in MOP receptor phosphorylation, desensitization and chronic opioid-induced adenylyl cyclase superactivation [31,34,35]. These indirectly characterized phospho-acceptor sites, if regulated in vivo, should represent minor species that are below the detection level of our MS analyses.

As illustrated above, studies in cellular models have helped understanding the role of phosphorylation in the regulation of MOP receptor activity but have also provided a large variety of data, depending on cells and methods used, which are sometimes difficult to reconcile, raising thus the question of their physiological relevance and highlighting the necessity to work closer to the native environment. Now that the proof of feasibility of applying semiquantitative label-free proteomic approach for analyzing in vivo MOP receptor phosphorylation is demonstrated, it will offer the opportunity to examine what happens in animals after acute and prolonged treatments with different classes of opioid drugs, upon heterologous regulation or in pathological conditions. Therefore, as a complement to the use of phosphosite-specific antibodies, the efficiency of which depends on their relative selectivity and affinity, in vivo proteomic approach is susceptible to provide a more quantitative and in-depth overview of the phosphorylation of native GPCR and paves the way for future exploration of other endogenous post-translational modifications.

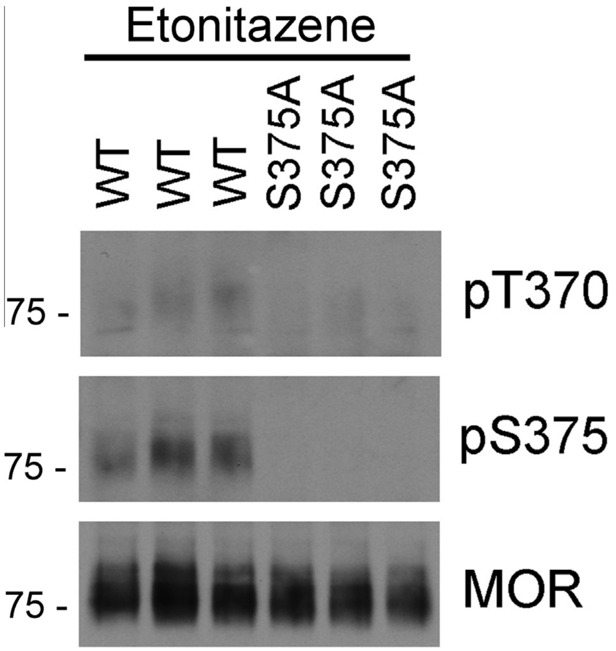

Fig. 5. Western blot image of UMB-3-immunopurified MOP receptor from brains of wild-type and phospho-deficient S375A MOP receptor mice injected (30 min, s.c.) with etonitazene 0.1 mg kg^{-1}. The blot was probed with anti-pT370 (first panel), anti-p375 (second panel) and with phosphorylation-independent anti-MOP receptor antibody.

Acknowledgements

This project was supported in part by the Région Midi-Pyrénées, European funds (Fonds Européens de Développement Régional, FEDER) and by the French Ministry of Research with the Investissement d'Avenir Infrastructures Nationales en Biologie et Santé program (ProFI, Proteomics French Infrastructure project, ANR-10-INBS-08).

References

[1] Chu, L.F., D'Arcy, N., Brady, C., Zamora, A.K., Young, C.A., Kim, J.E., Clemenson, A.M., Angst, M.S. and Clark, J.D. (2012) Analgesic tolerance without demonstrable opioid-induced hyperalgesia: a double-blinded, randomized, placebo-controlled trial of sustained-release morphine for treatment of chronic nonradicular low-back pain. Pain 153, 1583–1592.

[2] Law, P.Y., Reggio, P.H. and Loh, H.H. (2013) Opioid receptors: toward separation of analgesic from undesirable effects. Trends Biochem. Sci. 38, 275–282.

[3] Williams, J.T., Ingram, S.L., Henderson, G., Chavkin, C., von Zastrow, M., Schulz, S., Koch, T., Evans, C.J. and Christie, M.J. (2013) Regulation of mu-opioid receptors: desensitization, phosphorylation, internalization, and tolerance. Pharmacol. Rev. 65, 223–254.

[4] Krupnick, J.G. and Benovic, J.L. (1998) The role of receptor kinases and arrestins in G protein-coupled receptor regulation. Annu. Rev. Pharmacol. Toxicol. 38, 289–319.

[5] Butcher, A.J., Prihandoko, R., Kong, K.C., McWilliams, P., Edwards, J.M., Bottrill, A., Mistry, S. and Tobin, A.B. (2011) Differential G-protein-coupled receptor phosphorylation provides evidence for a signaling bar code. J. Biol. Chem. 286, 11506–11518.

[6] Liggett, S.B. (2011) Phosphorylation barcoding as a mechanism of directing GPCR signaling. Sci. Signal. 4, pe36.

[7] Nobles, K.N., Xiao, K., Ahn, S., Shukla, A.K., Lam, C.M., Rajagopal, S., Strachan, R.T., Huang, T.Y., Bressler, E.A., Hara, M.R., Shenoy, S.K., Gygi, S.P. and Lefkowitz, R.J. (2011) Distinct phosphorylation sites on the beta(2)-adrenergic receptor establish a barcode that encodes differential functions of beta-arrestin. Sci. Signal. 4, ra51.

[8] Tobin, A.B., Butcher, A.J. and Kong, K.C. (2008) Location, location, location...site-specific GPCR phosphorylation offers a mechanism for cell-type-specific signalling. Trends Pharmacol. Sci. 29, 413–420.

[9] Gluck, L., Loktev, A., Mouledous, L., Mollereau, C., Law, P.Y. and Schulz, S. (2014) Loss of morphine reward and dependence in mice lacking G protein-coupled receptor kinase 5. Biol. Psychiatry 76, 767–774.

[10] Chu, J., Zheng, H., Loh, H.H. and Law, P.Y. (2008) Morphine-induced mu-opioid receptor rapid desensitization is independent of receptor phosphorylation and beta-arrestins. Cell. Signal. 20, 1616–1624.

[11] El Kouhen, R., Burd, A.L., Erickson-Herbrandson, L.J., Chang, C.Y., Law, P.Y. and Loh, H.H. (2001) Phosphorylation of Ser363, Thr370, and Ser375 residues within the carboxyl tail differentially regulates mu-opioid receptor internalization. J. Biol. Chem. 276, 12774–12780.

[12] Doll, C., Konietzko, J., Poll, F., Koch, T., Hollt, V. and Schulz, S. (2011) Agonist-selective patterns of micro-opioid receptor phosphorylation revealed by phosphosite-specific antibodies. Br. J. Pharmacol. 164, 298–307.

[13] Chen, Y.J., Oldfield, S., Butcher, A.J., Tobin, A.B., Saxena, K., Gurevich, V.V., Benovic, J.L., Henderson, G. and Kelly, E. (2013) Identification of phosphorylation sites in the COOH-terminal tail of the mu-opioid receptor. J. Neurochem. 124, 189–199.

[14] Feng, B., Li, Z. and Wang, J.B. (2011) Protein kinase C-mediated phosphorylation of the mu-opioid receptor and its effects on receptor signaling. Mol. Pharmacol. 79, 768–775.

[15] Just, S., Illing, S., Trester-Zedlitz, M., Lau, E.K., Kotowski, S.J., Miess, E., Mann, A., Doll, C., Trinidad, J.C., Burlingame, A.L., von Zastrow, M. and Schulz, S. (2013) Differentiation of opioid drug effects by hierarchical multi-site phosphorylation. Mol. Pharmacol. 83, 633–639.

[16] Lau, E.K., Trester-Zedlitz, M., Trinidad, J.C., Kotowski, S.J., Krutchinsky, A.N., Burlingame, A.L. and von Zastrow, M. (2011) Quantitative encoding of the effect of a partial agonist on individual opioid receptors by multisite phosphorylation and threshold detection. Sci. Signal. 4, ra52.

[17] Mouledous, L., Froment, C., Dauvillier, S., Burlet-Schiltz, O., Zajac, J.M. and Mollereau, C. (2012) GRK2 protein-mediated transphosphorylation contributes to loss of function of mu-opioid receptors induced by neuropeptide FF (NPFF2) receptors. J. Biol. Chem. 287, 12736–12749.

[18] Doll, C., Poll, F., Peuker, K., Loktev, A., Gluck, L. and Schulz, S. (2012) Deciphering micro-opioid receptor phosphorylation and dephosphorylation in HEK293 cells. Br. J. Pharmacol. 167, 1259–1270.

[19] Johnson, E.A., Oldfield, S., Braksator, E., Gonzalez-Cuello, A., Couch, D., Hall, K.J., Mundell, S.J., Bailey, C.P., Kelly, E. and Henderson, G. (2006) Agonist-selective mechanisms of mu-opioid receptor desensitization in human embryonic kidney 293 cells. Mol. Pharmacol. 70, 676–685.

[20] Mann, A., Illing, S., Miess, E. and Schulz, S. (2014) Different mechanisms of homologous and heterologous mu-opioid receptor phosphorylation. Br. J. Pharmacol.

[21] Illing, S., Mann, A. and Schulz, S. (2014) Heterologous regulation of agonist-independent mu-opioid receptor phosphorylation by protein kinase C. Br. J. Pharmacol. 171, 1330–1340.

[22] Yousuf, A., Miess, E., Sianati, S., Du, Y.P., Schulz, S. and Christie, M. (2015) The role of phosphorylation sites in desensitization of mu-opioid receptor. Mol. Pharmacol.

[23] Schulz, S., Mayer, D., Pfeiffer, M., Stumm, R., Koch, T. and Hollt, V. (2004) Morphine induces terminal micro-opioid receptor desensitization by sustained phosphorylation of serine-375. EMBO J. 23, 3282–3289.

[24] Birdsong, W.T., Arttamangkul, S., Bunzow, J.R. and Williams, J.T. (2015) Agonist binding and desensitization of the mu-opioid receptor is modulated by phosphorylation of the C-terminal tail domain. Mol. Pharmacol.

[25] Lupp, A., Richter, N., Doll, C., Nagel, F. and Schulz, S. (2011) UMB-3, a novel rabbit monoclonal antibody, for assessing mu-opioid receptor expression in mouse, rat and human formalin-fixed and paraffin-embedded tissues. Regul. Pept. 167, 9–13.

[26] Grecksch, G., Just, S., Pierstorff, C., Imhof, A.K., Gluck, L., Doll, C., Lupp, A., Becker, A., Koch, T., Stumm, R., Hollt, V. and Schulz, S. (2011) Analgesic tolerance to high-efficacy agonists but not to morphine is diminished in phosphorylation-deficient S375A mu-opioid receptor knock-in mice. J. Neurosci. 31, 13890–13896.

[27] Petraschka, M., Li, S., Gilbert, T.L., Westenbroek, R.E., Bruchas, M.R., Schreiber, S., Lowe, J., Low, M.J., Pintar, J.E. and Chavkin, C. (2007) The absence of endogenous beta-endorphin selectively blocks phosphorylation and desensitization of mu opioid receptors following partial sciatic nerve ligation. Neuroscience 146, 1795–1807.

[28] Gautier, V., Mouton-Barbosa, E., Bouyssie, D., Delcourt, N., Beau, M., Girard, J.P., Cayrol, C., Burlet-Schiltz, O., Monsarrat, B. and Gonzalez de Peredo, A. (2012) Label-free quantification and shotgun analysis of complex proteomes by one-dimensional SDS–PAGE/NanoLC–MS: evaluation for the large scale analysis of inflammatory human endothelial cells. Mol. Cell. Proteomics: MCP 11, 527–539.

[29] Taus, T., Kocher, T., Pichler, P., Paschke, C., Schmidt, A., Henrich, C. and Mechtler, K. (2011) Universal and confident phosphorylation site localization using phosphoRS. J. Proteome Res. 10, 5354–5362.

[30] Maaty, W.S., Lord, C.I., Gripentrog, J.M., Riesselman, M., Keren-Aviram, G., Liu, T., Dratz, E.A., Bothner, B. and Jesaitis, A.J. (2013) Identification of C-terminal phosphorylation sites of N-formyl peptide receptor-1 (FPR1) in human blood neutrophils. J. Biol. Chem. 288, 27042–27058.

[31] Deng, H.B., Yu, Y., Pak, Y., O'Dowd, B.F., George, S.R., Surratt, C.K., Uhl, G.R. and Wang, J.B. (2000) Role for the C-terminus in agonist-induced mu opioid receptor phosphorylation and desensitization. Biochemistry 39, 5492–5499.

[32] Wang, H.L., Chang, W.T., Hsu, C.Y., Huang, P.C., Chow, Y.W. and Li, A.H. (2002) Identification of two C-terminal amino acids, Ser(355) and Thr(357), required for short-term homologous desensitization of mu-opioid receptors. Biochem. Pharmacol. 64, 257–266.

[33] Clayton, C.C., Bruchas, M.R., Lee, M.L. and Chavkin, C. (2010) Phosphorylation of the mu-opioid receptor at tyrosine 166 (Tyr3.51) in the DRY motif reduces agonist efficacy. Mol. Pharmacol. 77, 339–347.

[34] Wang, H., Guang, W., Barbier, E., Shapiro, P. and Wang, J.B. (2007) Mu opioid receptor mutant, T394A, abolishes opioid-mediated adenylyl cyclase superactivation. NeuroReport 18, 1969–1973.

[35] Wolf, R., Koch, T., Schulz, S., Klutzny, M., Schroder, H., Raulf, E., Buhling, F. and Hollt, V. (1999) Replacement of threonine 394 by alanine facilitates internalization and resensitization of the rat mu opioid receptor. Mol. Pharmacol. 55, 263–268.